Measuring Cerebrospinal Fluid Pressure With a Fluid Manometer

THESIS

Presented in Partial Fulfillment of the Requirements for the Degree Bachelors of Science in the Undergraduate School of The Ohio State University

By

Christian L. Blough

Undergraduate Program in Biomedical Engineering

The Ohio State University

2017

Thesis Committee:

Cynthia J. Roberts PhD, Advisor, and Robert H. Small MD

Abstract

A fluid manometer is the device of choice when measuring Cerebrospinal Fluid (CSF) pressure. CSF pressure can be an important indicator of certain pathologies of the body. CSF pressure is also relevant because it can be used as a surrogate for intracranial pressure. When measuring CSF pressure, a lumbar puncture is necessary, where a needle is used to gain access into the spinal canal. In theory the pressure reading should be taken after the fluid has stopped rising in the column, and equilibrium pressure is achieved between the spinal canal and the manometer. It has been hypothesized that the amount of time physicians wait to record CSF pressure may not be adequate for certain lumbar puncture needle gauges and types. To test this, a large fluid column was created above a port with a known height. The time to generate a fluid column in the manometer within 0.5 cm of the fluid height was recorded. This test was completed for many needles and a range of fluid column heights. The testing revealed that for certain needles, especially 25 Ga., 27 Ga., and 29 Ga., the time to record an accurate CSF pressure reading is quite long. Waiting more than 30 mins with a lumbar puncture needle inserted is not practical for the physician or patient. The results also showed that the method of measuring CSF pressure with a fluid manometer requires careful adherence to technique and knowledge of needle characteristics. These results are important because many published studies were based on data taken using fluid manometers, which may affect conclusions drawn from previous studies.

Acknowledgments

This project would not have been possible without the help of Cynthia Roberts, Robert Small, Ryan Somogye, and Rick Arnt. Funding was provided by the College of Engineering.

Vita

June 2013 …….McQuaid Jesuit High School

May 2017 …….B.S. Biomedical Engineering, The Ohio State University

Fields of Study

Major Field: Biomedical Engineering

Table of Contents

List of Tables

List of Figures

Chapter 1: Background and Introduction

A fluid manometer is a device that is often used to measure pressure in medical settings. The pressure is measured by reading the height of a fluid column in a graduated manometer. The measurement of fluid height is a good representation of fluid pressure once the level has stopped rising, and equilibrium has been achieved between the pressure in the manometer and the vessel that is being measured.

Manometers are the device of choice when measuring Cerebrospinal Fluid (CSF) pressure. CSF pressure can be an important indicator of certain pathologies of the body. CSF pressure is also relevant because it can serve as a surrogate for intracranial pressure (Lenfeldt, N., Koskinen, L., Bergenheim, A., et al., 2007). When measuring CSF pressure, a lumbar puncture is necessary, where a needle is used to gain access into the spinal canal. Once the needle is inserted into the spinal canal it is attached to the manometer and CSF fluid begins to flow through the needle and into the manometer. In theory, the pressure reading should be taken after the fluid has stopped rising in the column, and equilibrium pressure is achieved between the spinal canal and the manometer (Doherty & Forbes, 2014). The amount of time that it takes for equilibrium to occur depends on many factors. The biggest factor is the fluid flow rate through the spinal needle.

There are many differences in spinal needles used in medicine today. The gauge, the type of opening at the end, and the length are important factors that effect CSF flow through the needle that are available from the manufacturers. However, the inner diameter of the needle, which is related to the gauge, will likely be the most important factor affecting flow, but is not readily given by manufacturers. Depending on these variables, the time that it takes for an accurate CSF pressure reading to be reached can vary substantially. In practice, doctors might not wait long enough for full pressure equilibrium to be achieved.

The gauge and length of the needle used will have large effects on the time it takes to achieve pressure equilibrium. The reason for this is that laminar pressure driven flow of a Newtonian fluid through a cylinder has a direct relationship with diameter to the fourth power, and is inversely related to length. The Hagen-Poiseuille Equation, which is shown below, illustrates how flow rate, Q, is related to the change in pressure, ΔP, inner diameter of the cylinder, d, dynamic viscosity of the fluid, μ, and cylinder length, L.

$$Q = \frac{\Delta P * \pi * d^4}{128 * \mu * L}$$

With this in mind, the ideal spinal needle to conserve time would be one with a low gauge and short length. The issue with using low gauge needles is that this increases the risk of complications following the lumbar puncture (Lambert, D., Hurley, R., Hertwig, L., et al., 1997). This leaves a difficult decision for physicians performing lumbar punctures, and a decision that can very easily be debated from both sides; time is very important, but the risk of complications is also important and must be considered.

There is not a direct relationship between needle gauge and flow rate. The reason for this is that the gauge is only a measure of the outside diameter of the needle, not the inner diameter, and flow rate is a function of the inner diameter. Between two manufactures of the same gauge needle, the inner diameter may not be the same. This can have a large effect on the flow rate of the needle and the time it takes to reach pressure equilibrium. Another issue is that the manufacturer does not often give the inner diameter of a needle; frequently, only the gauge, length, and end type are given.

It has been hypothesized that what limits flow through spinal needles might be based on more than just inner diameter. In order to determine this and the flow characteristics through specific needles, the relationship between flow rate and needle gauge, length, and orifice will be investigated. Relationships will also need to be found for the time it takes to reach equilibrium pressure between the control vessel and the manometer based on needle gauge, length, and orifice. In collecting this information, the time required to achieve an accurate CSF pressure reading based on needle type and initial pressure will be determined.

Chapter 2: Materials and Methods

Fifteen spinal needles were obtained from The Ohio State University Department of Anesthesiology. The needles chosen are routinely used and represent a variety of gauges, lengths, and types. The specifics can be found in Table 1. Figure 1 shows some of the different types of needle orifices.

Manufacturer - Tip Design	Gauge	Length (mm)
BD Whitacre	22	90
Pajunk Sprotte	22	90
Pajunk Sprotte	22	150
B. Braun Pencan	22	90
BD Quincke	22	90
B. Braun Pencan	24	103
B. Braun Sprotte	24	90
Pajunk Sprotte	24	150
Pajunk Sprotte	24	120
B. Braun Pencan	25	127
BD Quincke	25	90
BD Whitacre	25	90
B. Braun Pencan	27	127
BD Whitacre	27	90
Pajunk Sprotte	29	90

Table 1: Needle Information

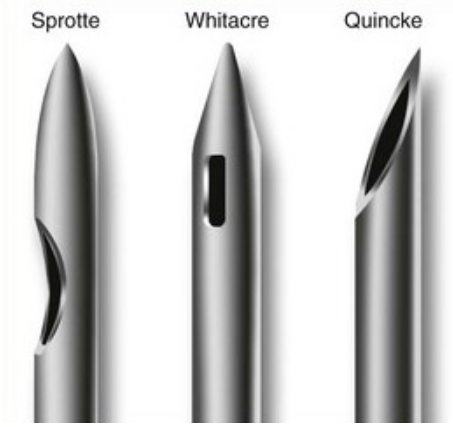

Figure 1: Needle orifices (Pencan not shown)

Once the needles were obtained, measurements were taken for the outer and inner diameter of each needle. To obtain the outer diameter a Mitutoyo Digital Micrometer was used that had a tolerance of 0.00005in. Measurements were taken at each end of the needle and in the center to assure that the outer diameter were consistent along the length of the needle. To obtain the inner diameter of the needles, a 24 Ga. 103 mm B. Braun Pencan, a 25 Ga. 127 mm B. Braun Pencan, and a 27 Ga. 127 mm B. Braun Pencan were cut in half using wire electrical discharge machining (EDM). Using Vermont Gage precision gage pins with a 0.0002inch tolerance, it was determined that the inner diameter was consistent along the length of the needle, and thus no more needles were cut. The precision gage pins were used to measure the inner diameters of all the needles by inserting the gage pin in the end of the needle where the connector is, except for the 29 Ga. 90 mm Pajunk Sprotte. No gage pin was small enough for this needle, so a measuring microscope was used that had a glass scale tolerance of 1 μm.

To create a fluid column of consistent height and consistent pressure, a hole was drilled in the side of a 5-gallon bucket. A 1.5 inch diameter PVC pipe was then inserted into this hole and sealed with a pipefitting and caulk. The other end of the PVC pipe was outfitted with an air port, a tee, and two elbows that terminated in 1 inch diameter threads. These connections were all sealed with pipe cement. To create a port that could be punctured by the needles repeatedly without spilling, medicine vials were sawed in half and pushed tightly over the threads that were covered with Teflon tape. This design can be seen in Figure 2.

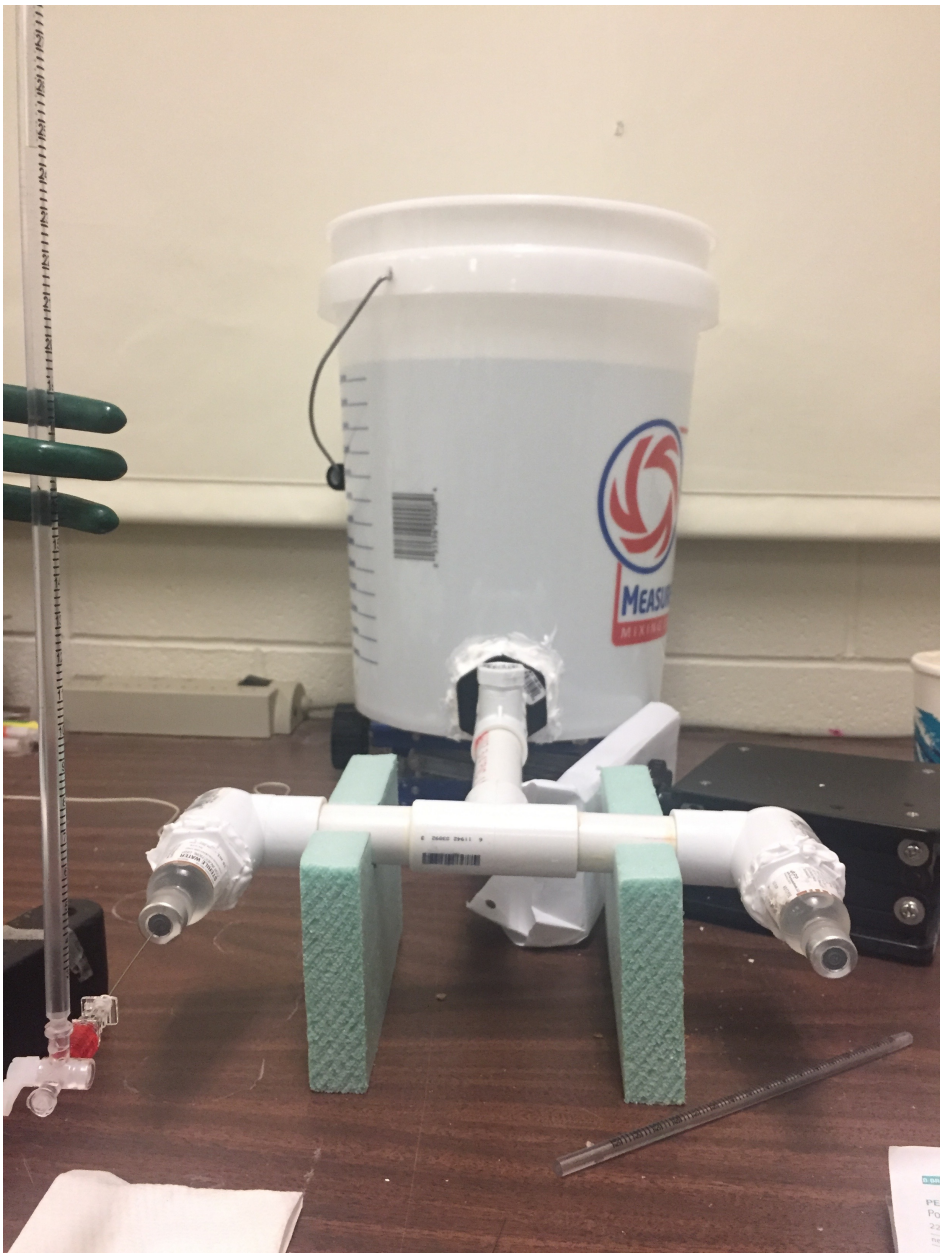

Figure 2: Fluid Column Setup

A computer simulation program was created in MATLAB to determine accurate predictions about the time it would take to reach equilibrium pressure between the bucket and manometer. The Hagen-Poiseuille equation was used to determine the instantaneous

flow rate through the needle. This flow rate was used to determine the increase in height of the fluid column in the manometer. A new flow rate and volume were calculated every hundredth of a second. When the fluid column heights were within 0.5 cm of the reference pressure, the simulation was stopped.

To obtain fluid flow measurements, distilled water was used to create the fluid column in the bucket. As the water was poured into the bucket, and the system was filling, the air port was opened to allow any air that might be trapped in the PVC piping or vials to escape. When the fluid column was of approximately the correct height, a needle was carefully inserted into the vial, ensuring that the entry was horizontal. The needle was then connected to the fluid manometer, which was held vertical at the proper height by a clamp connected to a ring stand. Once this setup was complete, a measurement was taken between the table and the needle's entry point into the vial. Another measurement was taken inner the bucket in the center to determine the height of the fluid, taking into account the meniscus. Since the height from the table to the bottom center of the bucket was known, taking these two measurements allowed for the fluid column height to be accurately adjusted to the desired level.

A strict protocol was followed for all trials. To begin, each needle was inserted into the vial with the stylet still inner. This was done to decrease the chance of any rubber from the vial entering the needle orifice, and to increase needle stiffness. Following insertion, the needle was rotated so that the key on the stylet was facing up. The stylet was then removed and the needle was connected to the manometer, keeping the key facing upwards. The manometer stopcock handle was then turned to vertical to allow for

fluid to flow through the stopcock without entering the manometer. This was done to remove all the air from the needle. Once a drop was observed leaving the stopcock, the handle was then turned to horizontal away from the needle allowing flow to begin to the manometer. The instant this turn was completed, the timer was started. The timer was stopped when the fluid column in the manometer was within 0.5 cm of the fluid column in the bucket.

With a fluid column of a known height created, multiple tests were completed on each needle. To determine if fluid flowed through the needles in an ideal fashion that could be accurately represented by the Hagen-Poiseuille equation, flow rate measurements were needed. These measurements were taken at a fluid column height of 10 cm of H_2O. To determine the flow rate, the fluid rising in the manometer was video recorded on an iPad. This was done to allow for many measurements to be taken of the height of the fluid column in the manometer at precise times. Once the videos were recorded and imported onto a computer, the software Wondershare Filmorama was used to zoom into the manometer and make accurate judgments of heights on the manometer. The time it took for the fluid to reach the heights of 3.0-9.8 cm of H_2O in 0.4 cm increments was recorded. Knowing the dimensions of the manometer and the elapsed time required for certain volume changes allowed the flow rate to be calculated at a range of pressure differences. From these data, a plot was created for each needle of flow rate vs. pressure difference. A least squared linear regression was then completed on each data set. The slope of this line should be equivalent to $\frac{\pi * d^4}{128 * \mu * L}$, or the inverse of the resistance of the needle. The slopes that were calculated from the trials were compared to

the theoretical values given the measured inner diameter, length, and dynamic viscosity. This was done to test the how well the Hagen- Poiseuille equation predicted fluid flow through the needles.

Following these trials, the time it took for equilibrium (within 0.5 cm of H_2O) to be reached between the fluid column in the bucket and the fluid column in the manometer was found. These measurements were taken to determine how long a physician would need to wait for accurate measurements to be taken when using a manometer to measure CSF pressure. This was completed for all needles at fluid column heights of 15 cm, 20 cm, and 25 cm of H_2O. The time it took for completion for a fluid column of 10 cm of H_2O was found on the videos taken for the flow rate measurements.

From the equilibrium testing trials the standard deviation was calculated to determine the variation in trials. T-tests were performed between the experimental data and the computer simulation to see if there was a statistical difference. A statistically significant difference was considered a p-value under 0.05.

Chapter 3: Results

Table 2 shows the results from the needle measurement testing.

Manufacturer - Tip Design	Gauge	Length (mm)	Listed ID (mm)	ID (mm)	OD (mm)	Listed OD (mm)
BD Whitacre	22	90	0.41	0.4191	0.720	0.72
Pajunk Sprotte	22	90	0.41	0.4572	0.700	0.72
Pajunk Sprotte	22	150	0.41	0.4699	0.706	0.72
B. Braun Pencan	22	90	0.41	0.5207	0.736	0.72
BD Quincke	22	90	0.41	0.4191	0.705	0.72
B. Braun Pencan	24	103	0.31	0.3937	0.589	0.57
B. Braun Sprotte	24	90	0.31	0.3302	0.548	0.57
Pajunk Sprotte	24	150	0.31	0.3302	0.550	0.57
Pajunk Sprotte	24	120	0.31	0.3175	0.546	0.57
B. Braun Pencan	25	127	0.26	0.3429	0.537	0.51
BD Quincke	25	90	0.26	0.2921	0.516	0.51
BD Whitacre	25	90	0.26	0.3048	0.515	0.51
B. Braun Pencan	27	127	0.21	0.2794	0.424	0.41
BD Whitacre	27	90	0.21	0.2794	0.429	0.41
Pajunk Sprotte	29	90	0.18	0.218	0.357	0.34

Table 2: Needle Measurements

Table 3 illustrates the results from the computer simulation that predicts the time for each needle to reach within 0.5 cm of the pressure in the bucket.

Manufacturer - Tip Design	Gauge	Length (mm)	10 cm H2O (sec)	15 cm H2O (sec)	20 cm H2O (sec)	25 cm H2O (sec)
BD Whitacre	22	90	178	203	220	233
Pajunk Sprotte	22	90	126	143	155	164
Pajunk Sprotte	22	150	188	214	232	246
B. Braun Pencan	22	90	75	85	92	98
BD Quincke	22	90	178	203	220	233
B. Braun Pencan	24	103	262	298	323	342
B. Braun Sprotte	24	90	463	526	570	605
Pajunk Sprotte	24	150	772	877	951	1008
Pajunk Sprotte	24	120	723	821	890	944
B. Braun Pencan	25	127	562	638	692	734
BD Quincke	25	90	757	859	932	988
BD Whitacre	25	90	638	725	786	833
B. Braun Pencan	27	127	1276	1448	1571	1666
BD Whitacre	27	90	904	1026	1113	1180
Pajunk Sprotte	29	90	2439	2769	3004	3185

Table 3: Computer Simulation Results

Figure 3 illustrates the flow rate calculations for a 10 cm fluid column with a 24 Ga. B. Braun Pencan 103 mm needle.

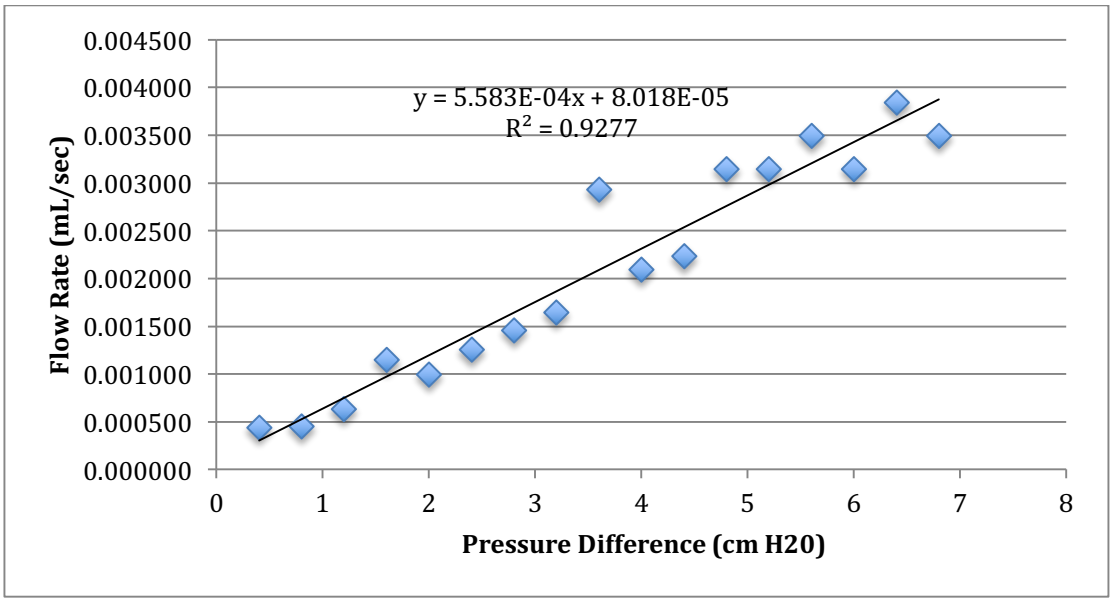

Figure 3: Plot of flow rate vs. pressure difference for 24 Ga. B. Braun Pencan 103 mm

Table 4 shows the results from flow rate tests and linear regression fitting for each needle. The expected column shows the predicted value of $\frac{\pi * d^4}{128 * \mu * L}$ based on the needle measurements and the dynamic viscosity of water at a temperature of 20 °C.

Manufacturer - Tip Design	Gauge	L (mm)	Slope (m^3/(s*Pa))	R2	Expected (m^3/(s*Pa))	Error
BD Whitacre	22	90	8.99E-12	0.978	8.38E-12	7.24%
Pajunk Sprotte	22	90	8.96E-12	0.949	1.19E-11	24.49%
Pajunk Sprotte	22	150	7.71E-12	0.954	7.95E-12	2.91%
B. Braun Pencan	22	90	2.07E-11	0.938	2.00E-11	3.57%
BD Quincke	22	90	8.59E-12	0.974	8.38E-12	2.57%
B. Braun Pencan	24	103	5.69E-12	0.928	5.70E-12	0.16%
B. Braun Sprotte	24	90	3.17E-12	0.949	3.23E-12	1.76%
Pajunk Sprotte	24	150	2.15E-12	0.883	1.94E-12	10.74%
Pajunk Sprotte	24	120	2.49E-12	0.905	2.07E-12	20.28%
B. Braun Pencan	25	127	2.95E-12	0.947	2.66E-12	10.81%
BD Quincke	25	90	1.83E-12	0.933	1.98E-12	7.23%
BD Whitacre	25	90	2.60E-12	0.918	2.34E-12	10.96%
B. Braun Pencan	27	127	1.19E-12	0.928	1.17E-12	1.70%
BD Whitacre	27	90	1.66E-12	0.948	1.66E-12	0.47%
Pajunk Sprotte	29	90	5.46E-13	0.967	6.13E-13	10.96%

Table 4: Results of flow rate testing at 10 cm H_2O

Table 5 shows the results from the equilibrium time tests

Manufacturer - Tip Design	Gauge	L (mm)	10 cm H20 (sec)	15 cm H2O (sec)	20 cm H2O (sec)	25 cm H2O (sec)
BD Whitacre	22	90	123 ± 4.4	142 ± 1.8	158 ± 1.9	163 ± 3.0
Pajunk Sprotte	22	90	90 ± 1.5	126 ± 2.8	134 ± 2.3	138 ± 1.9
Pajunk Sprotte	22	150	138 ± 2.6	212 ± 2.6	241 ± 1.8	243 ± 3.4
B. Braun Pencan	22	90	78 ± 2.5	62 ± 0.8	81 ± 0.7	85 ± 0.7
BD Quincke	22	90	123 ± 2.6	142 ± 0.9	143 ± 1.1	190 ± 2.4
B. Braun Pencan	24	103	154 ± 1.2	196 ± 2.2	197 ± 2.9	216 ± 1.5
B. Braun Sprotte	24	90	263 ± 4.6	330 ± 2.8	337 ± 2.5	377 ± 1.5
Pajunk Sprotte	24	150	428 ± 6.4	615 ± 5.3	564 ± 4.9	643 ± 6.6
Pajunk Sprotte	24	120	317 ± 3.8	483 ± 7.2	582 ± 4.6	670 ± 6.5
B. Braun Pencan	25	127	528 ± 4.6	403 ± 3.2	529 ± 2.8	638 ± 3.2
BD Quincke	25	90	477 ± 7.6	740 ± 5.1	759 ± 7.4	840 ± 4.0
BD Whitacre	25	90	332 ± 9.2	608 ± 5.2	577 ± 7.4	603 ± 2.8
B. Braun Pencan	27	127	750 ± 5.0	802 ± 5.4	958 ± 2.5	1235 ± 6.8
BD Whitacre	27	90	489 ± 3.6	579 ± 1.9	708 ± 2.1	916 ± 4.5
Pajunk Sprotte	29	90	1558 ± 14.1	1978 ± 7.9	2782 ± 14.2	2605 ± 12.2

Table 5: Equilibrium time test results

Table 6 below shows the percentage that the experimental results were of the computer simulation values.

Manufacturer - Tip Design	Gauge	Length (mm)	Computer Time 10 cm H2O (sec)	Actual Time 10 cm H20 (% of computer)	Computer Time 15 cm H2O (sec)	Actual Time 15 cm H20 (% of computer)	Computer Time 20 cm H2O (sec)	Actual Time 20 cm H20 (% of computer)	Computer Time 25 cm H2O (sec)	Actual Time 25 cm H20 (% of computer)
BD Whitacre	22	90	178	69.10%	203	69.85%	220	71.82%	233	69.79%
Pajunk Sprotte	22	90	126	71.43%	143	87.97%	155	86.19%	164	83.90%
Pajunk Sprotte	22	150	188	73.40%	214	98.88%	232	103.71%	246	98.94%
B. Braun Pencan	22	90	75	104.00%	85	73.18%	92	88.04%	98	86.73%
BD Quincke	22	90	178	69.10%	203	70.15%	220	65.18%	233	81.37%
B. Braun Pencan	24	103	262	58.78%	298	65.84%	323	61.11%	342	63.27%
B. Braun Sprotte	24	90	463	56.80%	526	62.70%	570	59.05%	605	62.38%
Pajunk Sprotte	24	150	772	55.44%	877	70.13%	951	59.26%	1008	63.75%
Pajunk Sprotte	24	120	723	43.85%	821	58.86%	890	65.37%	944	70.95%
B. Braun Pencan	25	127	562	93.95%	638	63.20%	692	76.47%	734	86.98%
BD Quincke	25	90	757	63.01%	859	86.15%	932	81.48%	988	85.06%
BD Whitacre	25	90	638	52.04%	725	83.86%	786	73.41%	833	72.41%
B. Braun Pencan	27	127	1276	58.78%	1448	55.40%	1571	60.96%	1666	74.12%
BD Whitacre	27	90	904	54.09%	1026	56.47%	1113	63.57%	1180	77.64%
Pajunk Sprotte	29	90	2439	63.88%	2769	71.43%	3004	92.62%	3185	81.79%

Table 6: Comparison of experimental results to computer simulation

Table 7 shows the results of the t-tests completed between the experimental results and the computer simulation. The values displayed are the calculated p-values.

Manufacturer - Tip Design	Gauge	L (mm)	10 cm H2O	15 cm H2O	20 cm H2O	25 cm H2O
BD Whitacre	22	90	2.10E-03	1.75E-07	1.99E-07	8.43E-07
Pajunk Sprotte	22	90	6.11E-04	1.57E-04	3.17E-05	7.08E-06
Pajunk Sprotte	22	150	9.32E-04	0.109	4.51E-04	0.166
B. Braun Pencan	22	90	0.208	4.34E-07	4.08E-06	2.09E-06
BD Quincke	22	90	7.70E-04	1.14E-08	1.18E-08	2.27E-06
B. Braun Pencan	24	103	3.79E-05	4.93E-08	6.64E-08	5.10E-09
B. Braun Sprotte	24	90	1.75E-04	9.60E-09	2.58E-09	4.73E-10
Pajunk Sprotte	24	150	1.16E-04	4.13E-08	6.29E-09	2.58E-08
Pajunk Sprotte	24	120	2.89E-05	4.92E-08	1.20E-08	7.74E-08
B. Braun Pencan	25	127	6.00E-03	8.21E-09	2.02E-08	3.04E-07
BD Quincke	25	90	2.49E-04	8.38E-07	8.25E-07	1.34E-07
BD Whitacre	25	90	3.03E-04	9.66E-07	3.87E-07	5.10E-09
B. Braun Pencan	27	127	3.06E-05	1.22E-09	5.63E-06	1.51E-08
BD Whitacre	27	90	2.52E-05	8.71E-11	2.40E-03	2.12E-08
Pajunk Sprotte	29	90	7.20E-03	2.33E-09	4.39E-06	4.67E-08

Table 7: t-test results

Chapter 4: Discussion

The listed outside diameters of the needles (Needle Gauge Chart), along with the results of the needle measurement test are displayed in Table 2. This shows that the measured outside diameters of all the needles fall within 5.5% of the listed outside diameter. This information tells us that the desired outside diameter can be found from the needle gauge. This is important because the larger the outside diameter of a needle, the higher the incidence of complications following lumbar puncture (Lambert, D., Hurley, R., Hertwig, L., et al., 1997). Having consistent outside diameters is important for physicians to minimize these complications by choosing the correct needle gauge.

The listed inner diameters of the needles (Needle Gauge Chart) shown in Table 2 are intended to be standard. The accuracy of these standards is unknown because manufacturers do not give the inner diameter. Table 2 shows that the measured inner diameters of many needles are different than the listed inner diameters. For example, the inner diameter of the 27 Ga. B. Braun Pencan 127 mm needle was measured to be 0.2794 mm. This is more than 33% larger than the listed inner diameter. One trend seen in the table is that all B. Braun Pencan needles have a larger inner diameter than listed as the standard. They all are more than 27% larger than expected. This could be important for a physician when choosing which needle to use because the flow rate of the needle is directly dependent on the inner diameter to the fourth power according to the Hagen-

Poiseuille Equation. This effect was previously studied, and it was shown that needles from different manufacturers of the same gauge and length had different flow rates.

The computer simulation created used the measured inner diameter, listed length, and the dynamic viscosity of water at 20 °C, which was found to be 1.002 mPa*s (Crittenden, Trussel, Hand, Howe, & Tchobanoglous, 2012). The room temperature of the lab was 20 °C, and the water was kept in the room so the temperature was assumed to be the same. The results shown in Table 3 match the expected trend; the higher gauge needles take significantly longer to reach a final pressure measurement. The 27 and 29 Ga. needles are predicted to take close to or above 20 minutes to achieve an accurate pressure measurement. This amount of time may not be clinically acceptable. Further complicating matters, the time varies significantly for different pressures, meaning that a recommendation cannot be made about a specific time that should be waited.

The characteristic plot of flow rate vs. pressure difference shown in Figure 3 represents the trend seen across all the needles tested. It was chosen to plot flow rate vs. change in pressure because both of these measurements should be easily calculated from the videos taken. The resulting slope of the linear regression done on this plot should be equal to $\frac{\pi * d^4}{128 * \mu * L}$, as previously stated. Given that the only variables in this slope are the inner diameter and length of the needle, comparing this calculated slope to the theoretical slope should show whether the fluid flow in the needle can be accurately predicted by the Hagen-Poiseuille Equation. As seen in Table 4, the linear regressions done on the data produced R^2 values almost exclusively within 0.07 of 1. The exception to this was the 24 Ga. Pajunk Sprotte 150 mm. These R^2 values indicate that the data does indeed follow a linear relationship between flow rate and change in pressure. The error between the

experimental slope and the theoretical slope was at or under 10% except for two needles, the 22 Ga. Pajunk Sprotte 90 mm, and the 24 Ga. Pajunk Sprotte 120 mm. The remainder of the needles have reasonably small errors, indicating that the fluid flow can be modeled by the Hagen-Poiseuille Equation, meaning the major factor that affects the flow rate is the inner diameter. A trend seen is that all but one of the Pajunk Sprotte needles has an error greater than or equal to 10%. This indicates that the limiting factor for the flow rate of the Pajunk Sprotte needle designs is not the inner diameter.

The results of the equilibrium tests shown in Table 5 follow many of the expected trends. The majority of needles had increasing time to equilibrate for increasing initialpressure difference. The exceptions to this trend were the 22 Ga. B. Braun Pencan 90 mm, the 25 Ga. B. Braun Pencan 127 mm, the 25 Ga. BD Whitacre 90 mm, and the 29 Ga. Pajunk Sprotte 90 mm. The standard deviation of all trials was below 4% of the measured value, indicating that the repeatability of the trials was quite high. This also indicates that the fluid flow is likely laminar. This agrees with the Reynolds Number calculations completed, which resulted in a maximum of 22, far less than a Reynolds Number of 2300 that is required to produce turbulent flow.

When comparing the results of the experimental equilibrium test to the theoretical computer simulation test, it is seen that the experimental tests give much shorter times to reach equilibrium. The comparison between the experimental results and the theoretical results can be found in Table 6. All experimental trials took less time than was predicted by the computer simulation, except for two trials. These two trials were the 22 Ga. Pajunk Sprotte 150 mm needle at 20 cm of H_2O, and the 22 Ga. B. Braun Pencan 90 mm needle at 10 cm of H_2O. These two trials had percentages slightly over 100%. Other needles

varied significantly from the expected time. For example the 24 Ga. Pajunk Sprotte 120 mm needle at 10 cm H_2O took less than 44% of the expected time to reach equilibrium.

The experimental trials were compared to the computer simulation via a t-test for each needle at each pressure. It was found that the experimental results were statistically different (p-value <0.05) from the computer simulation for all but three trials. These three trials were the 22 Ga. Pajunk Sprotte 150 mm needle at 15 and 25 cm of H_2O, and the 22 Ga. B. Braun Pencan 90 mm needle at 10 cm of H_2O. These results were not consistent with what was expected. A small portion of this error, at a maximum 5%, can be attributed to the uncertainty in the measurement of the inner diameter of the needle. All other sources of error except for two, would have led to experimental results that took longer than expected. These two sources of error were inaccurate measurement of the pressure difference, and the needles inner profile not being circular. Both of these sources could have resulted in experimental results that took longer or shorter than expected, but will be considered to have only made the experimental results shorter here. It was believed that this measurement was carried out correctly, and only small error should have resulted from human uncertainty in reading the manometer and height of the fluid column in the bucket. The computer simulation was modified to model a 0.1 cm error in both the height of the fluid column of the bucket and the reading of the manometer. For example, if the initial pressure was meant to be 10 cm of H_2O, the value was changed to 10.1 cm of H_2O in the simulation. The value that was considered to be equilibrium was also changed from 9.5 to 9.4 cm of H_2O. The simulation showed that these measurement errors would lead to a time to equilibrate error of around 10%. If the inner profile of the needles had been ovular instead of circular, the precision gauge pins used to measure

would have given the smallest diameter. This theory is thought to not be applicable though, as the needles that were cut for measurement were viewed under a microscope and the profile appears very circular.

In an attempt to determine the source of this larger error, many different scenarios were investigated, such as confirming the measurement marks on the manometer. A final concept was to confirm that the seemingly level table on which the experiment was placed, was in fact level. In doing this, it was determined that the table was slightly slanted, 1° from back to front. This does not seem like much, but given the design of the bucket and piping that delivers two ports, the ports are roughly 45 cm away from the point at which the height of the fluid column was measured. Depending on how far the needles were inserted into the ports, the distance from the measured fluid column height to the manometer could be around 50 cm in the direction of the slope. With this angle and length, the change in height would be around 0.87 cm. This change in height is quite dramatic, and when added to the computer simulation resulted in errors that were different and are shown in Table 8.

Manufacturer - Tip Design	Gauge	Length (mm)	Computer Time 10 cm H2O (sec)	Actual Time 10 cm H20 (% of computer)	Computer Time 15 cm H2O (sec)	Actual Time 15 cm H20 (% of computer)	Computer Time 20 cm H2O (sec)	Actual Time 20 cm H20 (% of computer)	Computer Time 25 cm H2O (sec)	Actual Time 25 cm H20 (% of computer)
BD Whitacre	22	90	123.4	99.68%	145.9	97.19%	162.2	97.41%	175	90.29%
Pajunk Sprotte	22	90	87.1	103.33%	103	122.14%	114.5	116.68%	123.5	108.18%
Pajunk Sprotte	22	150	130.2	105.99%	153.9	137.49%	171.1	140.62%	184.5	130.41%
B. Braun Pencan	22	90	51.8	150.58%	61.2	101.63%	68	119.12%	73.3	110.50%
BD Quincke	22	90	123.4	99.68%	145.9	97.60%	162.2	88.41%	175	81.94%
B. Braun Pencan	24	103	181.4	84.90%	214.5	91.47%	238.4	82.80%	257.2	76.75%
B. Braun Sprotte	24	90	320.4	82.08%	378.9	87.04%	421.2	79.91%	454.4	74.08%
Pajunk Sprotte	24	150	534	80.15%	631.5	97.39%	702.1	80.27%	757.4	74.41%
Pajunk Sprotte	24	120	499.7	63.44%	591	81.76%	657.1	88.54%	708.9	82.07%
B. Braun Pencan	25	127	388.7	135.84%	459.7	87.71%	511.1	103.54%	551.4	95.97%
BD Quincke	25	90	523.2	91.17%	618.7	119.61%	687.9	110.39%	742.1	102.33%
BD Whitacre	25	90	441.3	75.23%	521.9	116.50%	580.2	99.45%	625.9	92.19%
B. Braun Pencan	27	127	882	85.03%	1043.1	76.91%	1159.7	82.58%	1251.1	76.55%
BD Whitacre	27	90	625	78.24%	739.2	78.38%	821.8	86.09%	886.6	79.80%
Pajunk Sprotte	29	90	1686.5	92.38%	1994.6	99.16%	2217.6	125.47%	2392.5	116.30%

Table 8: Comparison of experimental results to updated computer simulation results

This fix still resulted in many of the experimental trials taking less time than expected, but the magnitude was smaller. Many of the trials error is now on the magnitude of being able to be mostly attributed to human measurement error and needle measurement error (~15%). Many of the needle trials now resulted in time longer than predicted by the simulation. There are many things that could have attributed to this type of error. If there was slight bend in the needle due to the insertion through the vial cap, this could have affected the fluid flow. This type of error may occur when inserting the higher gauge needles through skin and tissue. They are quite pliable and when the force for insertion is applied at a distance they bend quickly. Another source of positive error is the stopcock. In going through the stopcock the fluid flow direction changes from horizontal to vertical. This change in a short distance could disrupt the laminar flow. This source of error does not seem likely though, as all trials used the same stopcock.

The most likely reason for this error is very low flow rate as the pressure difference gets small. This can be seen in Figure 4.

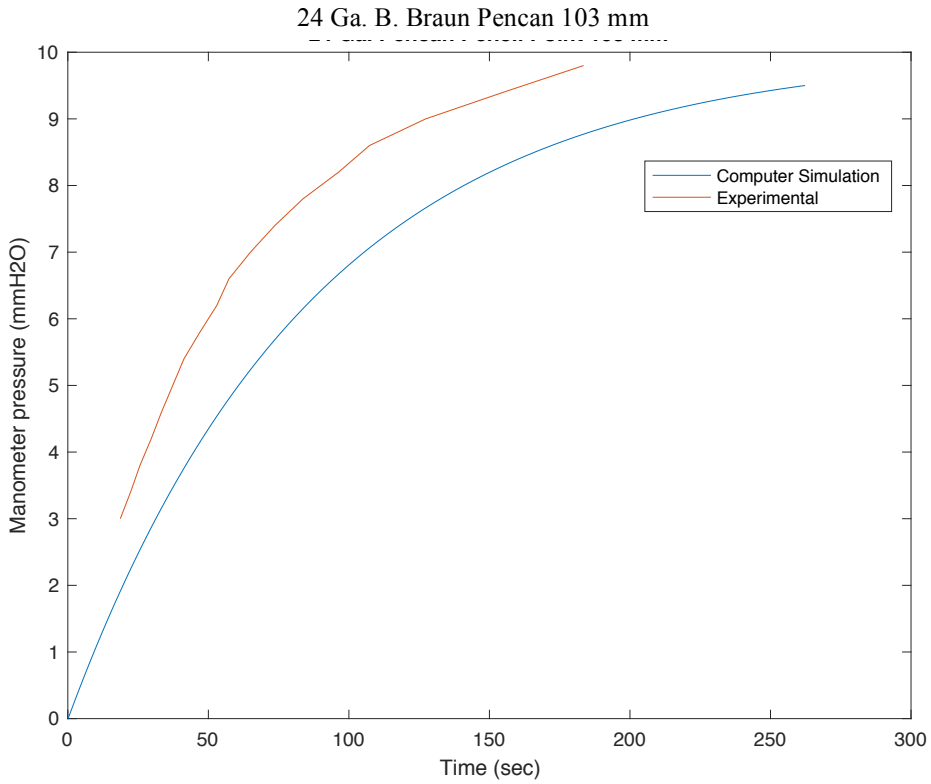

Figure 4: Plot of manometer pressure vs. time

The slope of these curves is the flow rate. It is seen that as the pressure difference nears zero, the slope becomes very small. This low flow rate means that a small error in the simulation or measurement of manometer height will have a large impact on the time to equilibrate. For example, as seen in the Figure 4, the time it takes the manometer pressure to change from 4 to 5 cm of H_2O is close to 15 seconds, while the time from 8 to 9 cm of H_2O is around 50 seconds.

A final consideration that needs to be made when comparing these results to what would be expected clinically is the fluid used. The dynamic viscosity of fluids varies with temperature. At body temperature, 37 °C, the dynamic viscosity of water is about 70% of

what it is at 20 °C (Crittenden, Trussel, Hand, et al., 2012). This is important to consider because flow rate is inversely related to dynamic viscosity meaning that the flow rate of water at body temperature would be roughly 30% greater than at 20 °C. The dynamic viscosity of CSF has previously been found to be in the range of 0.7 to 1.0 mPa*s, and not heavily effected by the concentration of solutes in the fluid. (Bloomfield, Johnston, & Bilston, 1998). These experimentally determined values of the dynamic viscosity of CSF are very similar to water, and therefore CSF can be appropriately modeled as water.

Chapter 5: Conclusion

This project investigated the time it takes to record an accurate pressure reading using spinal needles and a fluid manometer. A previous study was completed to determine the flow rate through needles at a constant pressure (Abouleish, E., Mitchell, M., Taylor, G., et al., 1994). Another study compared whether or not 20 and 22 Ga. needles gave pressure readings with a manometer that were 90% accurate after 1 min (Carson & Serpell, 1996). Because post-lumbar puncture headaches are prevalent with needles of this lower gauge (Lavi, Rowe, & Avivi, 2010), a study on needles of higher gauge is needed.

To determine whether or not the Hagen-Poiseuille Equation could model the flow, a computer simulation was created using the equation. Trials were then completed to determine if this simulation accurately represented the flow characteristics. These trials were completed at an initial pressure difference of 10 cm H_2O, and the results were compared to determine if the limiting factor of flow rate was the inner diameter of the needle. The results determined that the computer simulation could predict the flow rate with reasonable accuracy for most needles. The exception to this was most of the Pajunk Sprotte needles. This type of needle exhibited larger discrepancy from the simulation, meaning that the inner diameter might not be the biggest factor for flow rate. In this case the orifice at the end of the needle might be the limiting factor for flow rate.

The computer simulation was also used to determine the time it would take to reach an equilibrium pressure (within 0.5 cm H_2O), between the fluid column and the manometer. Experimental trials were completed at 10, 15, 20 and 25 cm of H_2O to determine if the computer simulation could accurately predict the time to equilibrate. It was found that the computer simulation could not accurately determine the time to equilibrate. This could have been due to a large number of factors, the most likely being the low flow rate at small pressure differences.

The equilibrium trials at different pressures show the unpredictability in measuring accurate pressures using a manometer. The results found were too inconsistent to determine the limiting factor in flow rate. The low flow rates through high gauge needles make the measurements difficult and more susceptible to human error. Because of this, it is recommended that if very accurate measurements of CSF pressure with a higher gauge needle are required, that a device other than a manometer is used.

References

Abouleish, E., Mitchell, M., Taylor, G., et al. (1994). Comparative flow rates of saline in commonly used spinal needles including pencil-tip needles. *Regional Anesthesia and Pain Medicine , 19* (1), 34-42.

Bloomfield, I., Johnston, I., & Bilston, L. (1998). Effects of Proteins, Blood Cells and Glucose on the Viscosity of Cebreospinal Fluid. *Pediatric Neurosurgery* , 246-251.

Carson, D., & Serpell, M. (1996). Choosing the best needle for diagnostic lumbar puncture. *Neurology , 47* (1), 33-37.

Crittenden, J., Trussel, R., Hand, D., et al. (2012). *MWH's Water Treatment: Principles and Design.* Hoboken, NJ: John Wiley & Sons, Inc.

Doherty, C., & Forbes, R. (2014). Diagnostic Lumbar Puncture. *Ulster Medical Journal , 83* (2), 93-102.

Lambert, D., Hurley, R., Hertwig, L., et al. (1997). Role of needle gauge and tip configuration in the production of lumbar puncture headache. *Regional Anesthesia and Pain Medicine , 22* (1), 66-72.

Lavi, R., Rowe, J., & Avivi, I. (2010). Lumbar Puncture: It Is Time to Change the Needle. *European Neurology , 64*, 108-113.

Lenfeldt, N., Koskinen, L., Bergenheim, A., et al. (2007). CSF pressure assessed by lumbar puncture agrees with intracranial pressure. *Neurology , 68* (2), 155-158.

Needle Gauge Chart. (n.d.). Retrieved 3 13, 2017, from Sigma-Aldrich: http://www.sigmaaldrich.com/chemistry/stockroom-reagents/learning-center/technical-library/needle-gauge-chart.html